RESEARCH ARTICLE

BON VIEW PUBLISHING

Improving Breast Cancer Diagnosis with AI Mammogram Image Analysis

Tiruveedula Gopi Krishna[1],* (ID) and Mohamed Abdeldaiem Abdelhadi Mahboub[2]

[1]Department of Computer Science and Engineering, School of Electrical Engineering and Computing, Adama Science and Technology University, Ethiopia

[2]Information Systems Department, Faculty of Information Technology, University of Tripoli, Libya

Abstract: Cancer is one of the worst diseases ailing humanity, but there is no known cure. Breast cancer is one of the most prevalent types of disease. Women aged 20–59 are disproportionately affected by breast cancer; however, death rates can be reduced with proper screening and treatment. Breast cancer detection and classification into cancer and healthy cells is one of the disease's most intractable difficulties. Cancer and healthy cells can be differentiated using AI methods based on their form and other biological features. This study proposes an artificial intelligence (AI)-enabled heuristic framework (AI-HF) with the Internet of Medical Things to identify and classify breast cancer at its earliest stages through machine intelligence techniques. The proposed method identifies cancer cells by extracting shape and texture-based features and then classifying them using machine learning classification techniques. Furthermore, this paper uses support vector machines to diagnose cancer based on optimal features taken from images of segmented cells. Experimental results on real datasets show that the suggested method accurately detects and classifies abnormal cells in breast cancer image rate of 98%. Finally, our AI-HF classifier is an efficient model that, in contrast to traditional techniques, can rapidly identify between cancer cells and healthy cells based on attributes extracted from images of the cells.

Keywords: breast cancer diagnosis, AI-powered image analysis, machine learning techniques, support vector machines, deep learning, CAD

1. Introduction

With one in eight cases worldwide, breast cancer is the primary cause of death for women. Enhancing survival rates requires early detection. While traditional techniques like ultrasound and mammography have their uses, they can be laborious and frequently require professional interpretation. Deep learning, a subset of artificial intelligence (AI), has shown promise in improving the diagnosis and prognosis of breast cancer. AI systems may be able to increase precision speed and efficiency by examining medical images. The intricacy of breast tissue and the scarcity of publicly available datasets however impede advancement. The goal of this review is to assess published research using machine learning techniques for breast cancer prognosis and diagnosis in a thorough manner. We can find chances to create AI-driven treatments for this illness that are more potent by analyzing the advantages and disadvantages of the approaches we currently employ [1–4]. Many medical imaging techniques are employed to analyze the human body for diagnosis, follow-up, or treatment. Determining whether surgery is required for a patient who has a positive biopsy is one example of how AI has the potential to transform the detection diagnosis and treatment of breast cancer [5, 6]. Imaging and physiological evaluations of computerized breast cancer diagnosis have greatly improved over the last five years thanks to the contributions of deep learning and convolutional networks [7]. A novel radiological technique called bioimaging quantification is being used in healthcare facilities more and more [8]. While MRIs don't pose any risks to patients, they do take longer and require extra care for those who have metal implants [9]. Although mammography is an important screening method for breast cancer, it is still difficult to segment the breast region effectively [10]. Automated technology is required because early detection through breast ultrasonography is critical, and there is a growing need for accurate and affordable screening [11]. Though its potential is limited by a lack of sufficient public training datasets, deep learning has recently been applied to enhance ultrasound-based breast cancer diagnosis [12].

Furthermore, novel signaling pathways and molecular structures linked to the prognosis of breast cancer have been discovered providing insights into tumorigenesis and metastasis [13]. Disease detection and monitoring with any given technology provide unique information regarding the area of the body being examined or treated, the nature of the disease or injury, or the results of any treatment administered [14]. The field of computer-aided design (CAD) focuses on locating suspicious lesions based on data generated by a computer. Radiologists are then responsible for determining the nature of the abnormalities and treating their patients accordingly. On the other hand, computer-assisted diagnosis uses human or computer detection results to determine the lesion's characterization and provide a malignancy likelihood and other anomalies [15].

*Corresponding author: Tiruveedula Gopi Krishna, Department of Computer Science and Engineering, School of Electrical Engineering and Computing, Adama Science and Technology University, Ethiopia. Emails: tiruveedula.gopi@astu.edu.et; gktiruveedula@gmail.com

Eliminating the challenge of interpreting data mining (DM) is the main purpose of a CAD system. DM interpretation and precise cancer diagnosis are among the systems' objectives but they are not the only ones. By lowering reliance on the operator for diagnosis, CAD structures were developed to decrease the cost of supplemental medical technology.

Eighty percent of diagnosed cells were detectable without CAD in the study on cancer cell detection by CADs. Still, inside CAD, the percentage of tested tumor cells detected by CADs increased to ninety percent [16].

We thought it would be useful to perform a comprehensive evaluation of published studies applying machine learning approaches in cancer diagnosis and prognosis in light of the rising importance of predictive medicine and the growing dependence on machine learning to make predictions.

Make sure your machine learning experiment is well-planned well-executed and fully validated to increase the odds of success [3]. CNN is a DL architecture with multiple layers. CNN is used to transform a picture's pixels into features. The characteristics are then used to classify and identify infections. Features are derived from the original photographs on CNN. The extraction process generates some irrelevant features from the raw images, which might harm the classification accuracy [17].

Traditional mammography, now known as full-field digital mammography (FFDM), consists of two 2D X-ray pictures of the breast taken by tech and analyzed by a radiologist to detect signs of breast cancer.

FFDM has been shown to have a significant effect on the death rate from breast cancer; regular screening has been linked to a decrease of more than 20 percent [18]. The diagnosis of disease in the field of surgical pathology is based only on microscopic images.

The groundbreaking advances in CAD and AI will have a significant influence on medical diagnosis in the future [19]. In place of artificial neural networks and Bayesian classifiers for the diagnosis and prognosis of breast cancer, SVM-based classifiers are a viable option. Distinguishing cancerous from non-cancerous, breast tumor is the main objective of diagnostics. If a patient has breast cancer, the tumor needs to be removed. After this procedure or any other postoperative procedure, an evaluation of the disease's anticipated course needs to be conducted [20].

The paper's primary contribution is as follows:

1) Proposes artificial intelligence-enabled heuristic framework (AI-HF) for the Internet of Medical Things (IoMT) with machine intelligence techniques (MIT) to become aware of and classify breast cancers at its earliest levels mentioned.
2) Machine learning classification strategies have been used to distinguish between most cancers and healthy cells.
3) Discussed applying AI methods like support vector machines (SVMs) to identify cancer cells based on their optimum features extracted from segmented images.

Coming sections are as follows: Section 2 discusses related works, Section 3 discusses materials and methods (AI-HF) for the net of clinical matters IoMT with MIT to perceive and classify breast cancer at its earliest degrees, Section 4 presents results and discussions, and Section 5 presents conclusion.

2. Related Works

To get around the current methods, the AI-HF was developed. It has been suggested by AI-HF to raise the ratios of performance accuracy sensitivity specificity efficiency and prediction in this research study development.

M. Desai et al. [21] proposed that a multilayer perceptron neural network (MLP) and a convolutional neural network (MLP-CNN) can be used to investigate the early detection of breast cancer in order to identify breast cell malignancies. To determine which network performed better, the diagnostic and classification accuracy of each one for breast cancer was examined. It has been shown that CNN is marginally more accurate than MLP at identifying and diagnosing breast cancer. Researchers took the same dataset and ran multiple analyses on it controlling for every possible variable to see if layout was more accurate. Nawaz and associates [22] presented the CNN model (DLBC-CNNM)-based deep learning approach for breast cancer classification. This method attempts to classify breast cancers as malignant or benign but it does not take into consideration the existence of tumor subtypes like lobular carcinomas and fibroadenomas. Experiments with histopathology images from the BreakHis dataset showed that the DenseNet CNN model outperformed state-of-the-art models in terms of processing presentation reaching a 95.4% accuracy rate when testing for multi-class breast cancer classification. Nilashi et coll. built a knowledge-based fuzzy rule set for classifying breast cancer subtypes (KbFRS) [23] and made use of the categorization and regression trees. They suggest applying principal component analysis in the knowledge-based system to address the multi-collinearity issue.

Experiments utilizing the Wisconsin Diagnostic Breast Cancer and Mammographic mass databases showed a significant improvement in prediction accuracy for breast cancer. The planned KbFRS was used as a CDSS to support physicians in their work. Jabeen et al. using deep learning and the integration of important features [24] presented a novel architecture for the classification of breast cancer from ultrasound images. The proposed method is divided into two main phases: (1) Improving CNN model learning by considering the classes in the enhanced dataset when adjusting the output layer of a pre-trained DarkNet-53 model (2) After the resulting model has been trained via transfer learning features are extracted from the global average pooling layer. A 96.1% best-case accuracy was achieved in testing using an improved dataset of breast ultrasound images. The suggested framework is better than more modern methods. Hirra [25] and others suggested using the Deep Belief Network (UP-DLA-DBN), a novel patch-based deep learning algorithm to identify and categorize breast cancer on histopathology images. A supervised tuning phase follows an unsupervised pre-training phase in which features are extracted. The proposed model was evaluated using a dataset that included all of the slides used in histopathology as well as images from four different data cohorts. It achieved an 86% accuracy rate. The model performs better in experiments than the previously suggested deep learning techniques proving the superiority of the suggested approach over the traditional ones. The current MLP-CNN DLBC-CNNM KbFRS and UP-DLA-DBN systems have trouble detecting and classifying images of breast cancer according to the survey. To get around the current methods, the AI-HF was developed. It has been suggested by AI-HF to raise the ratios of performance, accuracy, sensitivity, specificity, efficiency, and prediction.

3. Methodology

The AI-HF is explained in this section. A brief discussion of the research materials and methodology used in this paper is provided in the following subsections. Breast cancer strikes a disproportionately high percentage of women and is one of the leading causes of death globally. Early diagnosis led to a significant increase in breast cancer survival rates; today digital mammograms and histopathology scans

are considered the gold standards. It is recommended to use automatic diagnosis because human error can affect both the diagnosis and classification of breast cancer.

3.1. AI-enabled heuristic framework

This study proposes an AI-based method for breast cancer diagnosis using local binary patterns (LBP) and SVM. By analyzing over eighty studies and leveraging the IoMT, we developed a system capable of accurately classifying breast cancer based on histological image analysis, demonstrating effectiveness across various image conditions. The suggested approach makes use of mobile device capabilities in conjunction with AI system for classifying breast photos. A battery-operated portable AI-HF device is the first step. The proposed system employs a portable AI-HF device and a smartphone to classify breast images. The system uses a portable device and smartphone to capture and analyze breast images. The device's light adjusts to capture clear photos. Users take pictures of both breasts from different angles. Our current goal is to build a microcontroller that can detect breast cancer early by using a network of thermal micro-biosensors that are in direct contact with the breast. Thermal micro-biosensors are specialized sensors designed to measure minute temperature variations in biological tissues. In the context of breast cancer, they would be positioned in direct contact with the breast to detect subtle thermal anomalies associated with tumor growth. Microcontroller is the "brain" of the device. It processes the data collected by the micro-biosensors, analyzes it for patterns indicative of breast cancer, and potentially alerts the user or healthcare provider. This will enable us to leverage the experiences we had in this industry. CPU will enable data collection and transmission via the patient's smartphone to a dedicated server for the purpose of viewing the thermal picture and transmitting the diagnosis.

The creation of ovarian histopathology image features, extraction, the sliding window, building the classifier model, and finally image classification are all described in this section, along with the steps involved in the proposed system. Figure 1 displays a block diagram of the suggested computer system. The study includes LBP function extraction and the use of a sliding window technique. A greater thorough evaluation of the encouraged methods can be given within the resulting two subsections. When utilizing the sliding window approach, a window is moved throughout a microscopic histopathological photograph while keeping a size that falls between m and n. The chosen size should be proportionate to the size of the photo and no longer require 0 padding. Every aspect of the histopathological specimen's microscopic image will be carefully taken into account when this method is used. Moreover, Figure 1 classifier training incorporates a greater quantity of images. A microscopically rendered image of histopathology is used to illustrate the sliding window method. In this example, an image with 400 by 400 pixel resolution is displayed within a 50 by 50 pixel window.

3.1.1. Local binary pattern (LBP)

An example of LBP features for an image is illustrated in Figure 2. LBPs, commonly referred to as LBP, are among the most frequently used visual descriptors in computer vision and image processing for image classification. This is large because of the ease with which LBP can be computed. To put it simply, LBP
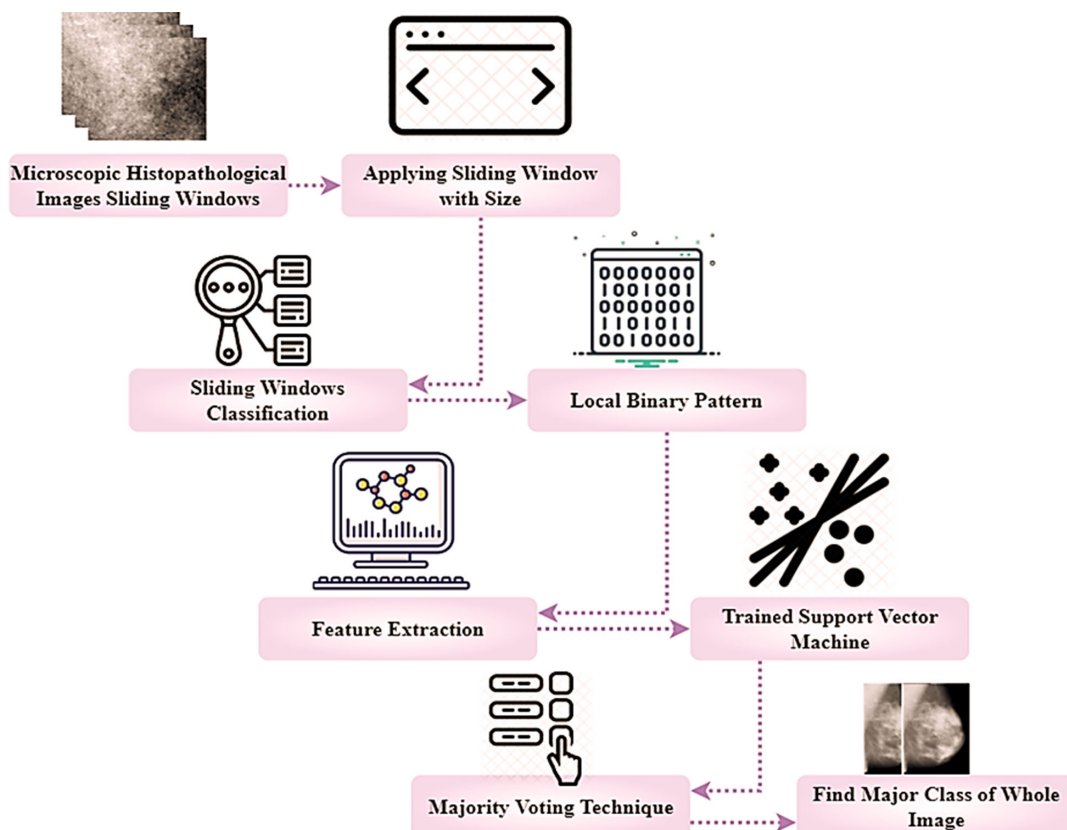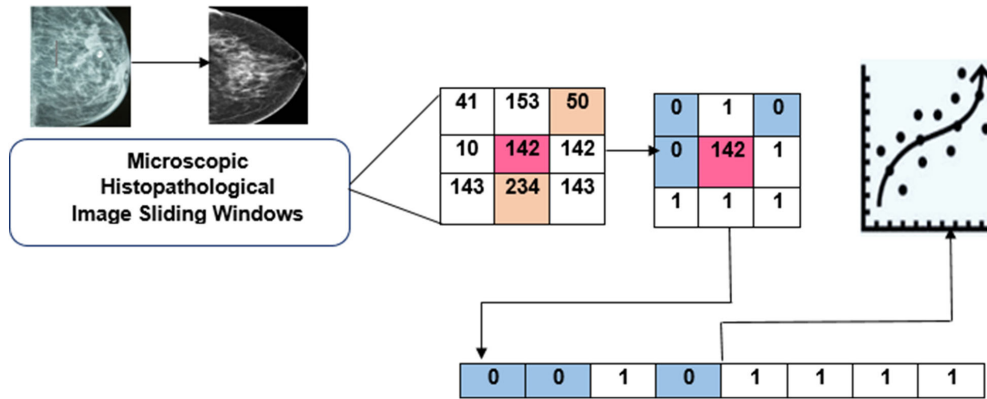

Figure 1. Proposed model architecture

Figure 2. Local binary pattern

is one of the most effective texture spectrum characteristics of the picture that is exploited. Once each pixel in an image has been tagged using an adapted threshold method, LBP will treat the result as a binary integer. This was how pixels in an image were named. The two qualities regarded as most valuable in the LBP technique are its robustness against changes in the monotonic gray level and its ease of computational implementation in practical applications. Real-time analysis of high-resolution images in challenging environments is made possible by these capabilities.

These microscopic images of the breast display a variety of cell types and other fluid-based objects as shown in Figure 2. Because of the images' high cell density, it could be difficult to identify the cell without any preprocessing. The input image uses the first MIT to increase the contrast between the foreground and background. Red, green, and blue components of the input picture have a strong correlation, which increases processing complexity when processing them. This gives the input image a new color space Lab where *a* and *b* represent the color dimensions and *K* stands for lightness. Lab colors improve image analysis for both the whole picture and specific areas. However, noise can make it difficult to identify features like cancerous cells. Filtering helps reduce noise, with non-linear filters like the median filter being a good choice for complex noise. But filter selection depends on the image and prioritizing noise reduction while keeping details sharp.

3.1.2. Image preprocessing

Preprocessing the image should be done to make it easier to identify abnormalities (cancers) without losing any important information. The breast region is included in mammograms, and it is positioned against backdrop structures that do not require further investigation. Limiting the investigation to the region of interest (ROI) which is the area of the picture without any background is one strategy. The initial preprocessing step in digital mammography entails separating the breast which is the area of interest from the backdrop which is frequently dark. The ROI is effectively separated from the dark backdrop using a thresholding technique. Think about input mammography against a dark background featuring a bright breast area. Coefficients for this mammogram are *f(yx)*. To separate the items from the background use the threshold value *S*. It is defined in Equation (1). When *e(yx)* is greater than *S* at a given location *(yx)*, the point is called the breast area; otherwise, it is called the

background region. The picture histogram is visually evaluated to establish the threshold.

$$J(y,x) = \{e, e(y,x) > s0, e(y,x) \le s \tag{1}$$

As shown in Equation (1), threshold value has been calculated for image preprocessing. A static examination of the saturation levels near each pixel is generated by examining the histogram of intensities and picking an appropriate threshold for the area. The average local intensity variations determine the boundary value. Breasts typically take up around 30% of the mammography image. Breast tissue is isolated and separated using this information for processing efficiency's sake.

The process of separating a picture into distinct pieces that do not overlap is referred to as image segmentation. The thresholding technique is one of the most accessible and valuable methods for separating a picture into items in the front and things in the background. The zone of interest (the foreground) in the input images is separated or discriminated from non-regions of attention or the backgrounds in this segment. The input image is converted from a gray level or colored image into a source image. The threshold value *t* is determined to separate the forefront from the background by decreasing the variation that occurs within each class when comparing the foreground to the background.

The optimum threshold provided by the AI-HF is derived by minimizing the intra-class variability (variation within the class), which is shown as a weighted combination of variations of the 2 classifications in the following Equation (2).

$$\delta_\tau^2 = \tau_0(s)\delta_0^2(s) + \tau_1(s)\delta_1^2(s) \tag{2}$$

As shown in Equation (2), δ_τ^2 is the combination of two weighted classifications that has been calculated, where *s* is the cutoff value, τ_0 and τ_1 stand for the two-class variances, and the weights δ_0^2 (*s*) and δ_1^2 correspond to the probability of the two classes. Some non-cell items remain once the binary picture is transformed and must be eliminated. Therefore, to reduce clutter from an input picture *J*, a structural element *N* performs the morphological closure operation, as described by the following equation:

$$J.N = (J \oplus N) \ominus N \tag{3}$$

As demonstrated in Equation (3), product value of the input image and structuring element value have been derived. The operator $\oplus$

represents a morphological enlargement, and the operator ⊖ represents a morphological reduction. However, area-based thresholding helps to remove noise even more effectively by eliminating most of the distracting elements in a picture.

3.1.3. Feature extraction

Correctly segmenting cell objects enables feature extraction from areas of interest, resulting in more accurate predictions. At the cellular level, the focus is primarily on the properties of individual cells. In order to perform classification on isolated objects, which contain little data and whose probability density functions are unknown, features are extracted using Gaussian Mixture, texture, and extra feature such as histogram gradients and wavelet. The proposed AI-HF extracts shape- and texture-based characteristics for identification and classification purposes.

Laws Texture Energy Measures (LTEM) are used to extract these texture characteristics from the ROI which includes abnormalities and standard tissue patterns. A tiny convolution kernel is first applied to the ROI to calculate these metrics, followed by a windowing procedure. The kernels are tailored to respond to edges, spots, lines, or combinations.

Convoluting a vertical 1-D kernel with a vertical 1-D kernel produces 25 unique 2-D convolution kernels. Similarly, 25 unique masks were created in only two dimensions. Once the preprocessed image (the ROI) has been applied with the two-dimensional mask, a collection of 25 $M \times N$ features, denoted by $E(i,j)$, will be obtained. The pixel-level LTEM is produced by applying a non-linear filter on $E(i,j)$. All of the neighboring pixels' absolute values are summed up. Here, a 15×15 square matrix is employed to fill in the areas outside of the texture's boundaries and other micro-features. The characteristics of a good non-linear filter are:

$$F(y, x) = \sum\nolimits_{i=-7}^{7} + \sum\nolimits_{j=-7}^{7} + |E(y + j, x + i)| \qquad (4)$$

As initialized in Equation (4), feature extraction has been discussed. This equation is then used to calculate the texture energy of each pixel in the ROI picture, yielding a total of 25 values. The texture characteristics found using the abovementioned equation are produced using zero-mean normalization. Finally, texture classification aims to produce a classification map of the input image, with labels for each region of the image that shares a single texture. Their nuclei's morphology defines different forms of cell differentiation. Several morphological parameters, including area, perimeter, anamorphic widescreen, sturdiness, eccentricities, form identity, the radius of curvature, compaction, extent, significant length, and minimal length, are retrieved from the nucleus because of its wide range of morphology. Below is a more in-depth explanation.

Nucleus area is the 2D image's area that is calculated by analyzing its nucleus pixel region. It expressed mathematically as:

$$B = \sum\nolimits_{v=1}^{n} + \sum\nolimits_{u=1}^{m} + t(v, u) \qquad (5)$$

As deliberated in Equation (5), nucleus area B has been evaluated, where B is the size of the nucleus and t is the n by m ROI defined by the segmentation and $t(v,u)$ is a segmentation range. The radius of curvature is the total distance between any two adjacent pixels that form the outside limit of the nucleus. Counting the number of edge pixels connected to the item is the quickest technique to get a sense of the nucleus's perimeter. The accompanying mathematical

equation proves it:

$$Q_j = \sum\nolimits_{n,m \in A_j}^{n} + T(n, m) \qquad (6)$$

As obtained in Equation (6), radius of curvature has been described, where Q_j is the perimeter, t is the picture with n columns and m rows removed to create an ROI, and A_j is the number of pixels that define the edge of the ROI. This quality is beneficial for distinguishing between circular and non-circular items or needle-like forms. Aspect ratios take on values between 0 and 1, inclusive. In this context, a number closer to 1 indicates more elongated cells (like cancerous ones), whereas a value closer to 0 indicates shorter cells.

The solidity of an ROI is defined as the area (b) of ROI divided by the area (d) of its convex hull. It is a crucial statistic that is calculated as follows:

$$Solidity = \frac{Area}{Convexhull} \qquad (7)$$

As computed in Equation (7), solidity has been expressed. The ratio of the squares of the surface and the radius is a quantitative measure of compactness. It determined by using the following formula:

$$Compactness = \frac{B}{Q^2} \qquad (8)$$

As evaluated in Equation (8), compactness has been evaluated. The parameters B and Q indicate the surface and the radius of the rectangle. It is a measurement of the circular reasoning of the chromosomes of the malignant cells, which indicates the degree to which the cell's nucleus is circular. The following is how it expressed mathematically:

$$Circularity = \frac{Q^2}{4\pi \times B} \qquad (9)$$

As expressed in Equation (9), circularity has been explored, where Q refers to the whole circumference. Between 0 and 1, the value of the circularity takes on various forms. If the nuclear curvature is equal to 1, then the form of the nucleus is characterized as circular elongation.

Cancer has a propensity to alter the chromosomes in the nucleus, which result in the nucleus taking on an abnormal form. This results in alterations in the circularity and roundness of the nucleus. The distance from the edge of the cancerous cell to the geographic center of the region is what is used to calculate roundness. In terms of computation, it expressed as the solution to the following equation:

$$Roundness = \frac{1 - \tau}{Distance} \qquad (10)$$

As obtained in Equation (10), roundness has been demonstrated. The deviation from the average distance is represented by the parameter 'height,' and τ is used in the following equations to calculate distances quantitatively.

$$\tau = \frac{\sqrt{\sum_{v,u}^{n} + (\|\varphi_0^t - t(v, u)\|)}}{Area} \qquad (11)$$

As calculated in Equation (11), distance has been identified, where φ_0^t represents the average value of the images in the size of a cell, and

$\Sigma(v,u)(\|\varphi_0{}^t\text{-}t(v,u)\|)$ represents the value of a single camera sensor in the space of a cell.

4. Support Vector Machine

SVMs are widely used in supervised machine learning for data classification into two groups. The SVM looks for the optimal hyperplane using the dataset as input and chooses it as the chosen one. SVM might be preferred for breast cancer classification when dealing with small to moderately sized datasets with high-dimensional data, where a clear margin of separation between classes exists. Decision Trees might be chosen when interpretability is paramount, but they might suffer from overfitting.

Random Forests offer a good balance of accuracy and robustness, especially for larger datasets, but they are less interpretable than SVMs and Decision Trees. One of the most important factors in selecting the optimal hyperplane should be extending the distance between the hyperplane and the data points that are closest to each class or group. The margin of error decreases as the categorization accuracy improves. SVM has been successfully applied to many different areas in the real world, such as recognizing digits, retrieving images, identifying emotions in faces, identifying medical images, and recognizing handwritten characters.

The proposed method used all of the characteristics as input data for radial-based function kernel SVM in order to identify benign microscopic histopathology pictures. Classification problems are frequently addressed by SVM a type of supervised machine learning.

The objective is to identify the hyperplane Z that most effectively separates the data into two groups: malignant and benign. The xi values of the dataset that lie closer to the hyperplane w are referred to as support vectors. The location of the hyperplane w is susceptible to the influence of these support vectors.

SVM performs better at classifying a data point when it is located far from the hyperplane. Transforming functions (as known as kernel functions L (yj,yi)) are used to move data from a lower-dimensional space $y_j \in O_m$ to a greater space Om (where $n > m$) so that linear segregation is performed. Using a kernel function allows for the implicit translation of datasets into higher dimensions without the need for additional memory and with minimal computational overhead. Various kernel functions, such as MLP, linear functions, polynomials, and quadratics, are available for application. The suggested method employs a cutoff value to determine whether cells are cancerous or benign. The following equation defines and provides the kernel for SVMs y_i and y_j in the input data.

$$L(y_j, y_i) = exp\left(-\frac{\|y_j - y_i\|}{2\sigma^2}\right) \tag{12}$$

As derived in Equation (12), Kernel function has been evaluated for SVM-based breast classification. Here, σ^2 is the free variable having a value higher than zero.

After the SVM, classifier has been trained and the classifier output class for each image window has been extracted from the sliding window LBP features the most frequent class is chosen as the value representing the class. With this strategy, we can predict both the window and slice levels. As was said before, the majority voting method helpful in the classification of categories across various degrees of magnification; hence, the classifier discriminates the characteristics differ depending on the magnifying level being used.

Information collecting comes initially, followed by specific data on breast cancer. Once the raw data on breast cancer have been collected, it is passed on to the preprocessing layer. Missing values in the raw data are addressed through the preprocessing layer, which serves as a crucial step. This layer also performs tasks such as applying moving averages and normalization techniques to prepare the data for analysis. Moving averages and normalization procedures are also carried out in the preprocessing layer. Using the standard portable has decreased the number of omissions and mistakes. After completing the layers that came before it, the preprocessing layer advances to the application layer.

The application layer includes both the performance assessment layer and the prediction layer. The elements that are thought to be essential for distinguishing between the different forms of breast cancer are given special attention in the prediction layer. Only the existence of an anomaly—that is whether a person is affected by the condition—is ascertained by the SVM. Figure 3 gives a graphic depiction of the two useful application layer strategies. Calculating accuracy and miss rate was done by the performance assessment layer. The current study suggests a system that would identify a particular heart condition by evaluating input data with the assistance of an MIT. To compute results based on the structure and behavior of neural networks, one can use a model called a SVM.
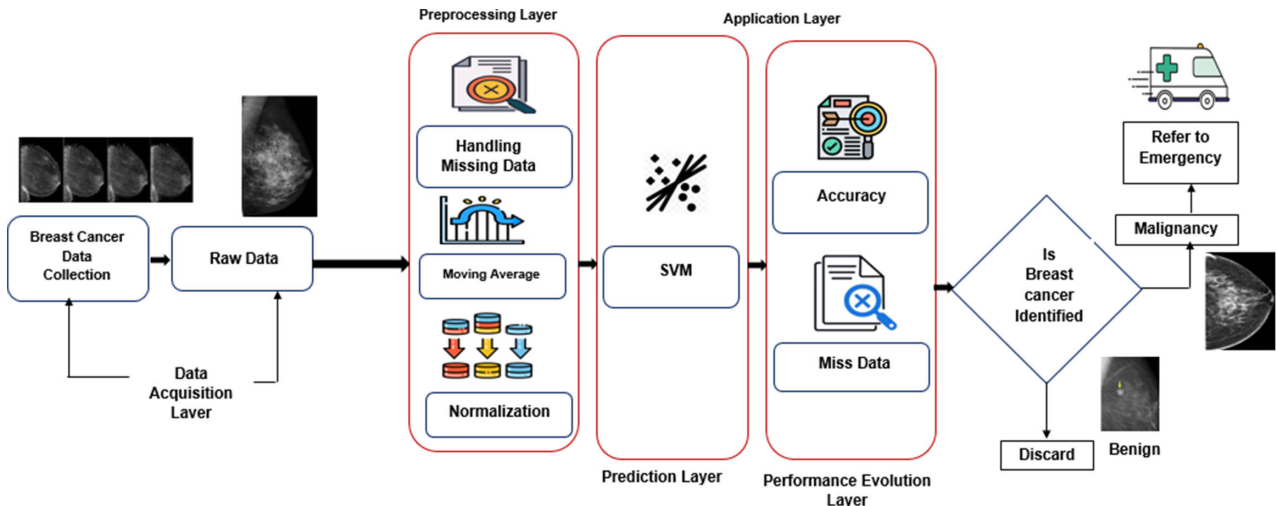

Figure 3. Identification of breast cancer classification using SVM

The results demonstrate its effectiveness in detecting cardiac disease. Additionally, the prediction layer utilizes an SVM model to diagnose breast cancer in patients. Patient's breast cancer is diagnosed using SVM in the prediction layer.

SVM is used for evaluation when examining the prediction layer output from the performance layer. Figure 3 displays the general workflow of the system including the input parameters that are part of the data collection layer. They will specifically use the neural system in this model, which calls for the use of a trained algorithm. SVM is used in industry and yields accurate results because of this.

SVMs use statistical modeling to analyze breast cancer data (30 input variables). This analysis helps classify whether cancer is present based on calculated precision and miss rates. This layer is a part of the field of statistical modeling, which studies the relationships between variables in a statistical model. The performance evaluation layer is responsible for calculating precision and miss rate. The determination as to whether or not breast cancer is present is reached in the region referred to as the crucial area.

This paper aims to show in future research that using this method, AI-HF ways to identify and classify breast cancer at its earliest stages. This will be proved by examining the prediction ratio, performance ratio, efficiency ratio, specificity ratio, accuracy ratio, and sensitivity ratio.

5. Results and Discussions

This research proposes a new method using IoMT and machine learning to identify breast cancer earlier. The method analyzes shapes and textures in mammogram images to categorize cells, potentially improving early detection rates.

Dataset Description: The purpose of this study is to build the first digitalized mammogram dataset for breast cancer in Saudi Arabia, based on the BI-RADS categories; this will help solve the availability problem of local public datasets by collecting, categorizing, and annotating mammogram images; this will support the medical field by providing physicians with a variety of diagnosed cases, particularly in Saudi Arabia. The dataset was obtained from the Sheikh Mohammed Hussein Al-Amoudi Center of Excellence in Breast Cancer at King Abdulaziz University in Jeddah, Saudi Arabia, during the months of April 2019 and March 2020, and the annotation process took place between the months of April and June 2020. The dataset has a total of 1416 cases, and each case contains pictures with two different kinds of views (CC and MLO) for both breasts (right and left). This results in a total of 5662 mammography images. Following the guidelines provided by BI-RADS, the dataset was divided into one of five distinct groups.

5.1. Model effectiveness: Prediction & performance (%)

To enhance breast cancer diagnosis prediction, we proposed a new AI-HF. Parametric in nature, our proposed system employs machine learning techniques to predict breast cancer in earlier stages. Without using any image enhancement techniques, our proposed framework performed 93.4% of the time according to the results as shown in Table 1. This indicates that our model performed better than the other MLP-CNN DLBC-CNNM KbFRS and UP-DLA-DBN approaches when we compare the results of the proposed method to those of these approaches. In comparison to a small number of well-known existing methods, segmentation techniques such as homomorphic filtering and feature extraction have improved AI-HF system performance. It has become possible to classify areas effectively and detect masses in mammograms. The traits that were discovered are divided into normal and abnormal groups. Our analysis of the performance of the proposed AI-HF method against other approaches from the literature indicates that our model works well.

5.2. Accuracy ratio (%)

The percentage of successes in making forecasts and a percentage of both negative and positive sample predictions are included. The formula for this is:

$$Accuracy = \frac{(TP + TN)}{(TP + TN + FP + FN)} \tag{13}$$

The true positives (TP) are the cancerous patches that the model correctly identifies; the false positives (FP) are the patches that are not the cancerous part but that the model identifies as cancer regions; the true negatives (TN) are the patches that are not cancerous and that the model correctly identifies as such, and the false negatives (FN) are the patches that are cancerous but that the model incorrectly identifies as such.

Comparing our method to other systems based on feature extraction from prior text our proposed system resulted in better accuracy. It is important to note that the sliding window methodology used in this method provides a vast database of subset pictures, which improves the classifier's ability to generalize and the accuracy with which it can be measured. Compared to systems in the literature, the proposed approach performs exceptionally well in terms of accuracy. Cancer, benign, and standard image were all correctly classified at an accuracy ratio of 92.4% using the AI-HF model.

5.3. Efficiency ratio (%)

A branch of AI that has arisen in the past decade has found many practical applications in the healthcare business and has yielded good outcomes at better efficiency. As seen by the findings, SVM achieved the best levels of accuracy across all picture types tested. To improve the categorization process's accuracy, selecting just the most relevant characteristics is necessary. Optimal characteristics extracted from cell segmentation pictures were used in an AI-HF for cancer classification. Our findings showed that the AI-HF with MIT had the most effective efficiency rate of any

Table 1. Comparisons of performance metrics

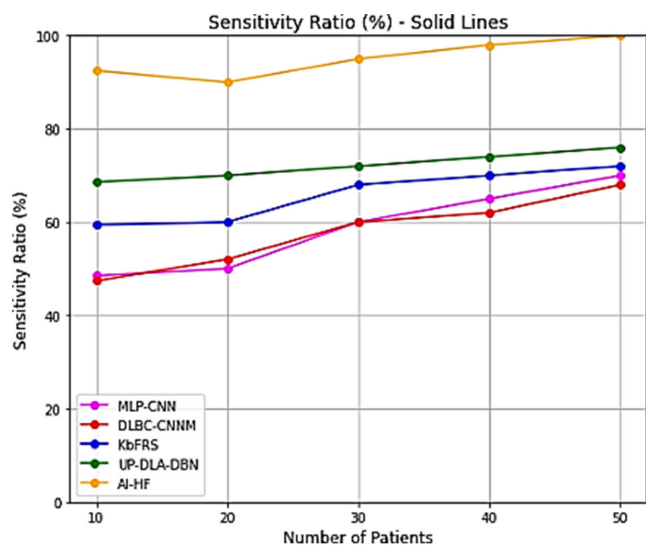|	Prediction ratio (%)	Performance ratio (%)	Accuracy ratio (%)	Efficiency ratio (%)	Sensitivity ratio (%)	Specificity ratio (%)
MLP-CNN	66.5	53.1	23.5	49.7	48.5	39.4
DLBC-CNNM	56.5	43.2	43.5	72.8	47.4	46.4
KbFRS	58.6	42.3	53.5	49.4	59.4	75.4
UP-DLA-DBN	54.6	53.1	51.4	60.5	68.6	49.9
AI-HF	93.4	92.5	92.4	93.7	92.5	96.3

Figure 4. Sensitivity ratio (%)

method (93.7%). In contrast to previously published methods, our AI-HF classifier was proven to be an appropriately trained model capable of quickly classifying cancerous and healthy cells utilizing cell image attributes. The results of our comparison between the proposed technique and other methods in the literature indicate that our model is superior.

5.4. Sensitivity ratio (%) and specificity ratio (%)

The efficiency of the FP reduction approach was demonstrated by proposing a methodology for mass identification in entire breast lesion images utilizing the symmetrical reduction process. This procedure identified six more significant masses on the analyzed images of aberrant breast tissue. A study found 83% sensitivity (5/6) with 13.8 FPs (165/12) per breast. See that the AI-HF system is relatively correct in Figure 4. The calculated precision is exceptional compared to other research contributions that have been analyzed. Sensitivity ratings closer to one another suggest fewer false negatives and a greater likelihood of detecting actual positives. The findings presented in Figure 5, based on real datasets, demonstrate the superiority of AI over SVM in classification
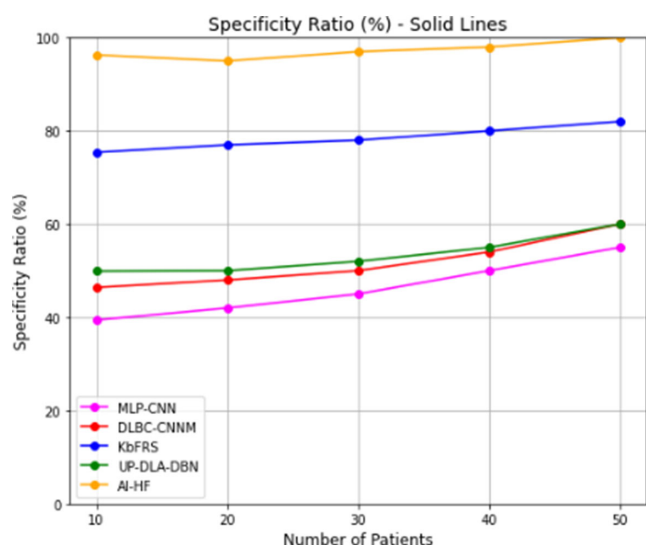

Figure 5. Specificity ratio (%)

accuracy, achieving rates as high as 98%. Incorporating AI-HF-based health care servers supporting IoMT for the proper categorization of various medical disorders would improve the suggested framework in the future, helping medical professionals make more informed judgments when detecting breast cancer. Compared to other models, the AI-HF's sensitivity and specificity are significantly higher (92.5% and 96.3%) than the MLP-CNN, DLBC-CNNM, KbFRS, and UP-DLA-DBN approaches.

Figure 4 illustrates the sensitivity ratio performance of AI-HF, DLBC-CNNM, and MLP-CNN across varying patient counts. AI-HF consistently outperforms the others, maintaining a high sensitivity ratio of over 90% throughout. DLBC-CNNM shows steady improvement with increasing patient numbers, reaching 70% sensitivity. MLP-CNN lags behind, with a final sensitivity of around 60%, highlighting its lower effectiveness in identifying relevant cases compared to the other methods. In summary, AI-HF is the highest-performing method, achieving sensitivity ratios above 90% across all patient counts, indicating strong reliability. DLBC-CNNM shows moderate performance with improvement as patient numbers increase, ending at 70%. MLP-CNN lags the most, achieving only about 60% sensitivity with 50 patients, showing limited effectiveness compared to the other methods.

Figure 5 illustrates the specificity ratio (%) for various methods (MLP-CNN, DLBC-CNNM, KbFRS, UP-DLA-DBN, and AI-HF) as the number of patients increases from 10 to 50. AI-HF consistently outperforms all other methods, maintaining specificity ratios close to 100% across patient counts, indicating its high effectiveness in correctly identifying TN cases. DLBC-CNNM shows moderate improvement, starting at around 80% specificity and reaching approximately 85% with 50 patients. KbFRS exhibits a similar trend to DLBC-CNNM, beginning near 55% and peaking at around 60% as patient numbers increase. UP-DLA-DBN, on the other hand, displays the lowest specificity ratio among the top methods, starting at about 40% and rising to roughly 50% with a larger patient sample. MLP-CNN maintains the lowest specificity overall, consistently below 50%, suggesting limitations in accurately identifying TN cases. In summary, AI-HF is the clear leader in specificity, DLBC-CNNM and KbFRS show moderate effectiveness, while UP-DLA-DBN and MLP-CNN have the lowest specificity, indicating challenges in correctly identifying TNs.

6. Conclusion

This study presents a novel classification scheme for the microscopic histological slices of breast tissue. The LBP is used to extract features from each window in the sliding window technique, allowing the system to initially discover local properties. Once the windows have been individually labeled, the final class is decided by a majority vote using a SVM. The suggested method solves the major problem of increasing the precision of breast categorization using histological sections. Compared to previous systems described in the research literature; the suggested system demonstrates superior performance in terms of accuracy. Moreover, the system is modified to improve accuracy by combining these characteristics with the extraction of more data from each frame. Prepare to examine the similarities and differences between various machine learning methods shortly. The numerical results show that the suggested method has a high accuracy ratio of 92.4%, a prediction ratio of 92.4%, a performance ratio of 91.8%, an efficiency ratio of 93.7%, a sensitivity ratio of 92.5%, and a specificity ratio of 96.3% than other existing methods. This research investigates a more vital prediction to improve breast cancer image accuracy.

Ethical Statement

This study does not contain any studies with human or animal subjects performed by any of the authors.

Conflicts of Interest

The authors declare that they have no conflicts of interest to this work.

Data Availability Statement

Data sharing is not applicable to this article as no new data were created or analyzed in this study.

Author Contribution Statement

Tiruveedula Gopi Krishna: Conceptualization, Methodology, Software, Validation, Formal analysis, Investigation, Writing – review & editing, Visualization, Project administration. **Mohamed Abdeldaiem Abdelhadi Mahboub:** Resources, Data curation, Writing – original draft, Supervision.

References

[1] Khan, S. U., Islam, N., Jan, Z., Din, I. U., Khan, A., & Faheem, Y. (2019). An e-Health care services framework for the detection and classification of breast cancer in breast cytology images as an IoMT application. *Future Generation Computer Systems*, *98*, 286–296. https://doi.org/10.1016/j.future.2019.01.033

[2] Alqudah, A., & Alqudah, A. M. (2022). Sliding window based support vector machine system for classification of breast cancer using histopathological microscopic images. *IETE Journal of Research*, *68*(1), 59–67. https://doi.org/10.1080/03772063.2019.1583610

[3] Kharya, S., Dubey, D., & Soni, S. (2013). Predictive machine learning techniques for breast cancer detection. *International Journal of Computer Science and Information Technologies*, *4*(6), 1023–1028.

[4] Heenaye-Mamode Khan, M., Boodoo-Jahangeer, N., Dullull, W., Nathire, S., Gao, X., Sinha, G. R., & Nagwanshi, K. K. (2021). Multi-class classification of breast cancer abnormalities using deep convolutional neural network (CNN). *PLOS ONE*, *16*(8), e0256500. https://doi.org/10.1371/journal.pone.0256500

[5] Abdollahi, J., Keshandehghan, A., Gardaneh, M., Panahi, Y., & Gardaneh, M. (2020). Accurate detection of breast cancer metastasis using a hybrid model of artificial intelligence algorithm. *Archives of Breast Cancer*, *7*(1), 22–28. https://doi.org/10.32768/abc.20207122-28

[6] Tahmooresi, M., Afshar, A., Rad, B. B., Nowshath, K. B., & Bamiah, M. A. (2018). Early detection of breast cancer using machine learning techniques. *Journal of Telecommunication, Electronic and Computer Engineering*, *10*(3–2), 21–27. https://jtec.utem.edu.my/jtec/article/view/4706

[7] Sechopoulos, I., Teuwen, J., & Mann, R. (2021). Artificial intelligence for breast cancer detection in mammography and digital breast tomosynthesis: State of the art. *Seminars in Cancer Biology*, *72*, 214–225. https://doi.org/10.1016/j.semcancer.2020.06.002

[8] Ortiz-Rodriguez, J. M., Guerrero-Mendez, C., Martinez-Blanco, M. D. R., Castro-Tapia, S., Moreno-Lucio, M., Jaramillo-Martinez, R., & Garcia, J. A. B. (2018). Breast cancer detection by means of artificial neural networks. In A. El-Shahat (Ed.), *Advanced applications for artificial neural networks* (Vol. 28, pp. 161–179). IntechOpen. https://doi.org/10.5772/intechopen.71256

[9] Nahid, A. A., & Kong, Y. (2017). Involvement of machine learning for breast cancer image classification: A survey. *Computational and Mathematical Methods in Medicine*, *2017*(1), 3781951. https://doi.org/10.1155/2017/3781951

[10] Patel, B. C., & Sinha, G. R. (2014). Abnormality detection and classification in computer-aided diagnosis (CAD) of breast cancer images. *Journal of Medical Imaging and Health Informatics*, *4*(6), 881–885. https://doi.org/10.1166/jmihi.2014.1349

[11] Inan, M. S. K., Alam, F. I., & Hasan, R. (2022). Deep integrated pipeline of segmentation guided classification of breast cancer from ultrasound images. *Biomedical Signal Processing and Control*, *75*, 103553. https://doi.org/10.1016/j.bspc.2022.103553

[12] Ayana, G., Park, J., Jeong, J. W., & Choe, S. W. (2022). A novel multistage transfer learning for ultrasound breast cancer image classification. *Diagnostics*, *12*(1), 135. https://doi.org/10.3390/diagnostics12010135

[13] Malherbe, K. (2021). Tumor microenvironment and the role of artificial intelligence in breast cancer detection and prognosis. *The American Journal of Pathology*, *191*(8), 1364–1373. https://doi.org/10.1016/j.ajpath.2021.01.014

[14] Houssein, E. H., Emam, M. M., Ali, A. A., & Suganthan, P. N. (2021). Deep and machine learning techniques for medical imaging-based breast cancer: A comprehensive review. *Expert Systems with Applications*, *167*, 114161. https://doi.org/10.1016/j.eswa.2020.114161

[15] Yassin, N. I., Omran, S., El Houby, E. M., & Allam, H. (2018). Machine learning techniques for breast cancer computer aided diagnosis using different image modalities: A systematic review. *Computer Methods and Programs in Biomedicine*, *156*, 25–45. https://doi.org/10.1016/j.cmpb.2017.12.012

[16] Zebari, D. A., Ibrahim, D. A., Zeebaree, D. Q., Haron, H., Salih, M. S., Damaševičius, R., & Mohammed, M. A. (2021). Systematic review of computing approaches for breast cancer detection based computer aided diagnosis using mammogram images. *Applied Artificial Intelligence*, *35*(15), 2157–2203. https://doi.org/10.1080/08839514.2021.2001177

[17] Jabeen, K., Khan, M. A., Alhaisoni, M., Tariq, U., Zhang, Y. D., Hamza, A., . . . , & Damaševičius, R. (2022). Breast cancer classification from ultrasound images using probability-based optimal deep learning feature fusion. *Sensors*, *22*(3), 807. https://doi.org/10.3390/s22030807

[18] Bai, J., Posner, R., Wang, T., Yang, C., & Nabavi, S. (2021). Applying deep learning in digital breast tomosynthesis for automatic breast cancer detection: A review. *Medical Image Analysis*, *71*, 102049. https://doi.org/10.1016/j.media.2021.102049

[19] Robertson, S., Azizpour, H., Smith, K., & Hartman, J. (2018). Digital image analysis in breast pathology—From image processing techniques to artificial intelligence. *Translational Research*, *194*, 19–35. https://doi.org/10.1016/j.trsl.2017.10.010

[20] Maglogiannis, I., Zafiropoulos, E., & Anagnostopoulos, I. (2009). An intelligent system for automated breast cancer diagnosis and prognosis using SVM based classifiers. *Applied Intelligence*, *30*, 24–36. https://doi.org/10.1007/s10489-007-0073-z

[21] Desai, M., & Shah, M. (2021). An anatomization on breast cancer detection and diagnosis employing multi-layer perceptron neural network (MLP) and convolutional neural network (CNN). *Clinical eHealth*, *4*, 1–11. https://doi.org/10.1016/j.ceh.2020.11.002

[22] Nawaz, M., Sewissy, A. A., & Soliman, T. H. A. (2018). Multi-class breast cancer classification using deep learning

convolutional neural network. *International Journal of Advanced Computer Science and Applications*, *9*(6), 316–332. https://doi.org/10.14569/IJACSA.2018.090645

[23] Nilashi, M., Ibrahim, O., Ahmadi, H., & Shahmoradi, L. (2017). A knowledge-based system for breast cancer classification using fuzzy logic method. *Telematics and Informatics*, *34*(4), 133–144. https://doi.org/10.1016/j.tele.2017.01.007

[24] Pattanaik, R. K., Mishra, S., Siddique, M., Gopikrishna, T., & Satapathy, S. (2022). Breast cancer classification from mammogram images using extreme learning machine-based

denseNet121 model. *Journal of Sensors*, *2022*(1), 2731364. https://doi.org/10.1155/2022/2731364

[25] Hirra, I., Ahmad, M., Hussain, A., Ashraf, M. U., Saeed, I. A., Qadri, S. F., . . . , & Alfakeeh, A. S. (2021). Breast cancer classification from histopathological images using patch-based deep learning modeling. *IEEE Access*, *9*, 24273–24287. https://doi.org/10.1109/ACCESS.2021.3056516